Virioplankton and virus-induced mortality of prokaryotes in the Kara Sea (Arctic) in the summer

Alexander Ivanovich Kopylov [Corresp., 1], **Elena Anatolyevna Zabotkina** [1], **Andrey Fedorovich Sazhin** [Corresp., 2], **Nadezhda Dmitriyevna Romanova** [2], **Nicolay Alexandrovich Belyaev** [2], **Anastasiya Nikolaevna Drozdova** [2]

[1] Papanin Institute for Biology of Inland Waters Russian Academy of Sciences, Borok, Yaroslavl region, Russia

[2] SHIRSHOV INSTITUTE OF OCEANOLOGY OF RUSSIAN ACADEMY OF SCIENCES, Moscow, Russia

Corresponding Authors: Alexander Ivanovich Kopylov, Andrey Fedorovich Sazhin
Email address: kopylov@ibiw.ru, andreysazhin@yandex.ru

Among the Arctic seas the largest volume of river runoff (~ 45 % of the total inflow of river waters into the Arctic Ocean) enters the Siberian Kara Sea. The Kara Sea viral communities are important for sea ecosystem functioning. The studies of the virus-prokaryote interactions in the riverine - marine waters on the Kara Sea shelf were conducted only in the spring and autumn. Here, we investigated the structure and abundance of virioplankton, viral infection and virus-mediated mortality of prokaryotes in early summer, i.e. during the period of ice melting and the inflow of maximum volumes of river water with a high concentration of dissolved and suspended organic carbon. Seawater samples for microbial analyses were collected across the shelf zone of the Kara Sea on board the vessel *Norilskiy Nickel* as a research platform from June 29 to July 15, 2018. Abundances of prokaryotes (range (0.6–25.3) × 10^5 cells mL^{-1}) and free viruses (range (10–117) × 10^5 viruses mL^{-1}) were correlated ($r = 0.63$, $p = 0.005$, $n = 18$) with an average virus : prokaryote ratio of 7 (range 4–35). Free viruses with a capsid diameter of 16−304 nm were registered in the water samples examined. Waters in the Kara Sea shelf contained high concentrations of suspended organic particles (PD) with a size of 0.25−4.0 μm (range (0.6–25.3) × 10^5 particles mL^{-1}. The proportions of free viruses, viruses attached to bacteria and viruses attached to the pico-sized detrital particle were 89.8±6.0 %, 2.2±0.6 % and 8.0±1.3 %, respectively of the total virioplankton abundance (on average (61.5±6.2) × 10^5 viruses mL^{-1}). Using transmission electron microscopy, we estimated that an average 1.4% (range 0.4–3.5%) of the prokaryote community was visibly infected with viruses which suggest that a substantial proportion of prokaryotic secondary production was lost due to viral lysis. There was a negative correlation between the abundance of PD and the frequency of visibly infected prokaryotic cells $r = -0.67$, $p = 0.0008$, $n = 18$. The abundance of free viruses and viral-mediated mortality of prokaryotes were significantly

higher in summer than in early spring and autumn.

Virioplankton and virus-induced mortality of prokaryotes in the Kara Sea (Arctic) in the summer

Alexander I. Kopylov[1*], Elena A. Zabotkina[1], Andrey F. Sazhin[2**], Nadezhda D. Romanova[2], Nicolay A. Belyaev[2], Anastasia H. Drozdova[2]

[1] *Papanin Institute for Biology of Inland Waters of the Russian Academy of Sciences, Borok, Yaroslavskaya oblast, Russia*

[2] *Shirshov Institute of Oceanology of the Russian Academy of Sciences, Moscow, Russia*

***e-mail:*

Subjects: Ecology, Marine Biology, Hydrobiology, Microbiology

Corresponding author *: Alexandr Kopylov
109, Borok, Nekouzsky district, Yaroslavl region, 152742, Russia
E-mail address: kopylov@ibiw.ru
Corresponding author **: Andrey Sazhin
36, Nakhimovskiy prospect, Moscow, 117997, Russia
E-mail address: andreysazhin@yandex.ru

ABSTRACT

Among the Arctic seas the largest volume of river runoff (~ 45 % of the total inflow of river waters into the Arctic Ocean) enters the Siberian Kara Sea. The Kara Sea viral communities are important for sea ecosystem functioning. The studies of the virus-prokaryote interactions in the riverine - marine waters on the Kara Sea shelf were conducted only in the spring and autumn. Here, we investigated the structure and abundance of virioplankton, viral infection and virus-mediated mortality of prokaryotes in early summer, i.e. during the period of ice melting and the inflow of maximum volumes of river water with a high concentration of dissolved and suspended organic carbon.

Seawater samples for microbial analyses were collected across the shelf zone of the Kara Sea on board the vessel *Norilskiy Nickel* as a research platform from June 29 to July 15, 2018. Abundances of prokaryotes (range (0.6–25.3) $\times 10^5$ cells mL^{-1}) and free viruses (range (10–117) $\times 10^5$ viruses mL^{-1}) were correlated ($r = 0.63$, $p = 0.005$, $n = 18$) with an average virus : prokaryote ratio of 7 (range 4–35). Free viruses with a capsid diameter of 16−304 nm were registered in the water samples examined. Waters in the Kara Sea shelf contained high concentrations of suspended organic particles (PD) with a size of 0.25−4.0 μm (range (0.6–25.3) $\times 10^5$ particles mL^{-1}. The proportions of free viruses, viruses attached to bacteria and viruses attached to the pico-sized detrital particle were 89.8±6.0 %, 2.2±0.6 % and 8.0±1.3 %, respectively of the total virioplankton abundance (on average (61.5±6.2) $\times 10^5$ viruses mL^{-1}). Using transmission electron microscopy, we estimated that an average 1.4% (range 0.4–3.5%) of the prokaryote community was visibly infected with viruses which suggest that a substantial proportion of prokaryotic secondary production was lost due to viral lysis. There was a negative correlation between the abundance of PD and the frequency of visibly infected prokaryotic cells $r = -0.67$, $p = 0.0008$, $n = 18$.

The abundance of free viruses and viral-mediated mortality of prokaryotes were significantly higher in summer than in early spring and autumn.

Key words: Viruses, prokaryotes, virioplankton, viral infection, Kara Sea, Arctic.

LIST OF ABBREVIATIONS

PD – particles of pico-sized detritus
N_{PD} – abundance of particles of pico-sized detritus
N_{PDV} – abundance of particles of pico-sized detritus with attached viruses
N_{PR} – abundance of prokaryotes
N_{PRV} – abundance of prokaryotes with attached viruses
V_{PR} – volume of prokaryotic cell
B_{PR} – biomass of prokaryotes
N_{VF} – abundance of free viruses
N_{VPR} – abundance of viruses attached to prokaryotic cells
N_{VPD} – abundance of viruses attached to particles of pico-sized detritus
D_{VF} - capsid diameter of free viruses
FVIC – frequency of visibly infected prokaryotic cells
N_{PRVIC} – abundance of visibly infected prokaryotic cells
FIC – frequency of infected prokaryotic cells
VMPR – viral-mediated mortality of prokaryotes
BS – burst size

INTRODUCTION

Studies conducted in different Arctic regions have demonstrated that viruses are the most numerous component of the plankton community and play a significant role in the functioning of microbial communities in cold waters, as well as in marine waters of temperate and tropical climates (Middelboe, Nielsen & Bjørnsen, 2002; Hodges et al., 2005; Wells & Deming, 2006a; Suttle, 2007; Maranger et al., 2015; Sandaa et al., 2018). In Polar Regions viruses maintain their infectivity at low temperatures (Middelboe, Nielsen & Bjørnsen, 2002; Weinbauer, Brettar & Höfle, 2003) and viral lysis can be important in controlling prokaryotic abundance (Guixa-Boixereu et al., 2002; Wells & Deming, 2006b). Viral lysis of prokaryotes may also influence the composition of the prokaryotic community (Weinbauer & Rassoulzadegan, 2004) and trigger the release of intracellular material upon lyses, which in turn stimulates the cycling of dissolved organic carbon (DOC) by heterotrophic prokaryotes (Bratbak, Thingstad & Heldal, 1994; Wilhelm & Suttle, 1999; Suttle, 2007).
Coastal marine systems in the Arctic typically contain high concentrations of inorganic and organic particles which enter the water column via melting of land and sea ice and via large river run-off (Lasareva et al., 2019; Maat, Prins & Brussaard, 2019). The high suspended particle load may substantially reduce the ability of viruses to infect prokaryotes as viruses are efficiently adsorbed by silt, clay, organic particles (Murray & Jackson, 1992; Simon et al., 2002). The Kara Sea is mostly a shallow Arctic shelf basin influenced by the river runoff. The Kara Sea receives 1300-1400 km^3 of fresh water annually, which accounts for 41% of total freshwater runoff to the Arctic Ocean (Makkaveev et al., 2015). About 40% of the Kara Sea area is influenced by the water masses of the Ob and Yenisei rivers entering the eastern part of the sea, which are most pronounced in summer. Previously, it was shown that the structural and functional characteristics of planktonic prokaryotes in the Kara Sea shelf areas adjacent to the estuaries of the Ob and Yenisei rivers are largely determined by the impact of their river runoff (Kopylov et al., 2017; Romanova & Boltenkova, 2020; Romanova et al., 2022).
In recent years, data have been obtained on the abundance of planktonic viruses and virus-mediated mortality of prokaryotes in different areas of the Kara Sea shelf in early spring and

autumn (Kopylov et al., 2015, Kopylov et al., 2019). At the same time, virioplankton and viral infections of heterotrophic prokaryotes in the Kara Sea in the phenological period of late spring and early summer remain unstudied.
Our central aim of the present study was to determine the abundance of free viruses, viruses attached to prokaryotic cells and the pico-sized detrital particles, the size structure of free viruses and virus-mediated mortality of prokaryotes (*VMPR*) on the Kara Sea shelf during early summer. A secondary aim was to evaluate the differences in the structure of virioplankton and viral infection of prokaryotes in the marine waters of the western part of the sea (Marine Area, MA) and coastal desalinated waters of the eastern part of the sea influenced by the runoff of the Ob and Yenisei rivers (Coastal Area, CA).

MATERIALS & METHODS

Study sites and sampling

Water samples were collected from June 29 to July 15, 2018 on board the vessel *Norilskiy Nickel* at 21 stations along the vessel's course from the station in the Barents Sea near the Kara Strait to the station near the Taimyr Peninsula in the Yenisei estuary and back to the Kara Strait. Stations were located in the shelf area that does not receive river runoff (MA) and in the shelf area adjacent to the estuaries of the Ob and Yenisei rivers (CA) (Fig. 1). Samples at stations 3 and 4 were taken in the ship-made channels in the water area completely covered with ice; stations 5, 24 and 25 were located in open water among the ice fields. Other stations were ice-free.
Temperature was measured using the SBE-39 probe and LCD-thermometer (HANNA Checktemp-1). Salinity (in Practical Salinity Scale) was measured using a Kelilong PHT-028 salinity meter (China). Surface water samples for biological variables and dissolved organic carbon (DOC) were collected with a sterile 10-L bucket container from the side of the ship by hand. The DOC concentrations were measured using Shimadzu TOC-Vcph carbon analyzer coupled to a SSM-5000A solid sample modulee (Belyaev, Peresypkin & Ponyaev, 2010).
Water samples for microscopic studies were fixed immediately after sampling with 25% glutaraldehyde (final concentration 1%). Samples for determining the abundance and biomass of prokaryotes were stored in the dark at 2−4°C until the end of work at the station, after which preparations to be examined to luminescent microscopy were prepared. Preparations were stored at -24ºC for 1 month before analysis.
Samples for the study of viruses were subsequently stored at -80ºC until processing at home laboratory.

Enumeration of prokaryotes and of smallest organic particles

The abundances of prokaryotes (cocci and ellipsoids, rods and vibrios, filaments were estimated separately) were determined by standard techniques using the fluorochrome 4', 6'–diamidino–2–phenylindole (DAPI) and epifluorescence microscopy (Porter & Feig, 1980). From each station a 7 ml sample stained with DAPI at a 1 μg mL^{-1} (final concentration) and filtered onto a black nuclepore filter (0.2 μm pore size). Filters were placed on glass slides and covered with immersion liquid Leica Typ N and cover glass.
Observation and counts were made under an epifluorescent microscope (Leica DM 5000 B) at a magnification of × 1000 in two replicates. On each filter, at least 400 prokaryotes were counted and the dimensions of at least 100 cells were measured. The wet biomass was estimated based on the individual cell volume using Image Scope Color image analysis software. The carbon

content in prokaryotic cells (C, fg C cells^{-1}) was calculated using the following allometric equation: $C = 120 \times V^{0.72}$, where V is the mean volume of prokaryotic cells, μm^3 (Norland, 1993).
Yellow pico-sized organic particles (0.25 to 4.0 μm in size), which were clearly distinguished from prokaryotic cells, were also counted, as well as prokaryotes, on DAPI-stained filters by epifluorescence microscopy (Porter & Feig, 1980; Mostajir et al. 1995; Wells & Deming, 2003). On each filter, at least 400 of smallest detrital particles were counted.

Enumeration of viruses

The viral particles were counted under an epifluorescent microscope using SYBR Green I fluorochrome and Whatman Anodisc aluminum oxide membrane filters (pore size 0.02 μm) (EM) (Noble & Fuhrman, 1998). Depending on the viral abundance, between 0.2 and 1.0 mL of water was poured onto the Anodisc filters. Counts were done under an Olympus BX51 epifluorescent microscope (Olympus, Japan) using Cell F Image Analysis Software at ×1000 magnification. For each water sample, two filters were analyzed; counts yielded a minimum of 800 viruses. The carbon content in the viral particles was taken as 0.055 fg C virus^{-1} (Steward et al., 2007).
Concurrently, viruses were counted and their sizes were determined using transmission electron microscopy (TEM) (Suttle, 1993; Bettarel et al., 2000). Viruses were identified on the basis of morphology (round or hexagonal capsid structures, tailed and non-tailed), size and staining characteristics. The following six classes of virus capsid size were examined to characterize viral populations: <40, 40−60, >60−100, >100−150, >150−200 и >200 nm. In addition, we measured the proportion of prokaryotic cells with attached viruses of the total prokaryotic abundance, the proportion of smallest detrital particles with attached viruses of the total abundance of pico-sized detrital particles with a size of 0.25−4.0 μm, the abundance of viruses attached to a single prokaryotic cell and to a single detrital particle. No less than 800 detrital particles were analyzed per sample

Viral-infected prokaryotes and subsequent mortality

Transmission electron microscopy was used to estimate the frequency of visibly infected cells (*FVIC*, estimated as the share (%) of total prokaryotic abundance), the mean number of fully matured phages in prokaryotes (i.e., burst size (*BS*), viruses cell^{-1}). In glutaraldehyde-fixed samples, the viruses, prokaryotes and smallest detrital particles contained in 50-ml samples were harvested by centrifuging onto Pioloform/carbon-coated 400-mesh nickel grids, using OPTIMA L-90k ultracentrifuge (Beckman Coulter, USA) at 100,000 × g for 2 h. Two grids were thus prepared for each water sample.
The grids were then positively stained at room temperature with 1% aqueous solutions of uranyl acetate and lead citrate. The grids were further analyzed under a JEM 1011 electron microscope (Jeol, Japan) at ×50 000–150 000 magnification. At least 1200 prokaryotic cells per sample were examined to determine the frequency of visibly infected cells (*FVIC*). Cells were scored as infected if they contained four or more intracellular viruses. For each sample, the mean burst size (viruses prokaryotes^{-1}) was estimated.
Because viruses inside prokaryotic cells become visible during the last ~10% of the lytic cycle (Proctor, Okubo & Fuhrman, 1993), FVIC were converted to the frequency of infected prokaryotes (*FIC*) using the equation: $FIC = 7.1 \times FVIC - 22.5 \times FVIC^2$ (with data given as percentages) (Binder, 1999). Assuming a steady state, that the infected and uninfected

prokaryotes were grazed at the same rate, and that the latent period equaled the bacterial generation time, FIC were converted to viral-mediated mortality of prokaryotes (*VMPR*, as a percentage per generation, i.e., assuming that *VMPR* equals the losses of prokaryotic production) using the equation (Binder, 1999): $VMPR = (FIC + 0.6 \times FIC^2)/ (1 – 1.2 \times FIC)$.

Statistical analyses

Correlations between the parameters were analyzed using to the Pearson's correlation coefficient calculated by Past 4.03 software (Hammer et al., 2001) and regarding the prerequisites for the data analyzed.

RESULTS

Environmental Parameters

The temperature of the surface water layer at the station in the Barents Sea adjacent to the Kara Strait was higher than at the station in the Kara Strait and on the Kara Sea shelf (Table 1). The average water temperature in MA (1.6±0.4ºC) was 3 times lower than that in CA (5.2±1.7ºC) and the salinity, on average for the area, in MA (30.69±0.50 psu) was 2.8 times higher than in CA (10.80±2.69 psu). The concentration of dissolved organic carbon (DOC) in CA water (on average, 8.57±0.58 mg L^{-1}) exceeded that in MA water (on average, 2.28±0.10 mg L^{-1}) by 3.8 times.

Abundance of prokaryotes and of pico-sized organic particles

The abundance (N_{PR}) and biomass (B_{PR}) of prokaryotes varied widely in the surface water layer (Table 1). The minimum and maximum N_{PR} and B_{PR} values differed by 39 and 34 times, respectively. The highest values were recorded in the eastern part of CA (stations 12, 18). During the periods June 29–July 1 and July 12–15, there was no significant difference between average N_{PR} values in MA (1.7±0.4 × 10^5 cells mL^{-1} и 2.0±0.2 × 10^5 cells mL^{-1}, respectively) and in CA (12.3±2.7 × 10^5 cells mL^{-1} и 10.5±2.0 × 10^5 cells mL^{-1}, respectively). As a result, over the entire period (June 29–July 15), N_{PR} and B_{PR} were on average 7.6 × 10^5 cells mL^{-1} and 7.82 mg C m^{-3} in the Barents Sea, 1.8±0.4 × 10^5 cells mL^{-1} and 2.36±0.38 mg C m^{-3} in MA, and 11.4±2.4 × 10^3 cells mL^{-1} and 12.15±2.60 mg C m^3 in CA. The average cell volume of prokaryotes was 0.034 μm^3 in the Barents Sea, 0.042 μm^{-3} in the Kara Strait, 0.049±0.004 μm^3 in MA, 0.035±0.002 μm^3 in CA. High positive correlations were found between N_{PR} and water temperature ($r = 0.84$, $p < 0.00001$, $n = 18$) and between N_{PR} and DOC ($r = 0.75$, $p = 0.00037$, $n = 18$). There was a significant inverse relationship between N_{PR} and salinity ($r = -0.74$, $p < 0.00002$, $n = 18$).

The amount of the pico-sized organic particles was significant in the studied waters. These yellow pico-sized particles are pico-sized detritus (PD) (Mostajir, Dolan & Rassoulzadegan, 1995; Wells & Deming, 2003). The abundance of detrital particles of 0.25−4.00 μm (N_{PD}) varied between 1.75 and 20.59 ×10^5 particles mL^{-1}. The average N_{PD} value in MA (8.7±1.7)×10^5 particles mL^{-1} was lower than in CA (12.5±2.3)×10^5 particles mL^{-1} by 1.4 times.

Abundance of virioplankton and composition

In the shelf zone of the Kara Sea, enumeration of viruses by EM and TEM did not reveal significant differences (t = 40 – 2.03, p = 0. 21, as determined by t test). The epifluorescence microscopy estimates of free viral concentrations ranged from 10 ×10^5 viruses mL^{-1} to 117 ×10^5 viruses mL^{-1} (Table 2, Fig. 2). The N_{VF} values in the Barents Sea and the Kara Strait were lower than in MA (on average, 50±6 × 10^5 viruses mL^{-1}) and CA (on average, 68±10 × 10^5 viruses mL^{-}

^{1}). The average N_{VF} values in MA and CA in the period of June 29−July 1 were higher by 1.3 times than in the period of July 12−July 15. The N_{VF}/N_{PR} ratio in MA (on average 37.0±7.2) was significantly higher than in CA (on average 7.6±1.7). As a result, in the summer, the average N_{VF} and N_{VF}/N_{PR} values on the Kara Sea shelf constituted 55±6 × 10^5 viruses mL^{-1} and 22.4±5.0, respectively.

There was a high positive correlation between N_{VF} and N_{PR} (r = 0.63, p = 0.005, n = 18) in surface waters on the Kara Sea shelf.

The capsid diameter (D_{VF}) of free viral particles varied from 16 to 304 nm (Table 2). The average capsid diameter values varied between 37 and 64 nm per water sample, averaging 50±7 nm for 21 samples. The average D_{VF} values in MA and CA were close, 53±2 nm and 51±2 nm, respectively. On the Kara Sea shelf, the fraction of viruses with the size of <40, 40−60, >60−100, >100−150, >150−200 and >200 nm of the total virioplankton abundance was on average 40.54±14.85, 36.89±6.21, 18.67±10.26, 3.11±2.71, 0.64±1.09 and 0.15±0.37%, respectively for all water samples. Thus, in the period of June 29–July 15, 2018, viruses with a capsid diameter of ≤60 nm amounted to 77.43% of the total abundance of free viruses.

The abundance of prokaryotes with viruses attached to their cells (N_{PRV}) varied within (0.2−11.2) × 10^5 cells mL^{-1} (on average 1.60±51 × 10^5 cells mL^{-1}), that was 10.9-40.7% (on average 24.0±1.4) of the total abundance of prokaryotes (Table 3, Fig. 2). There was from 1 to 12 viral particles attached to the surface of a cell of prokaryotes. From 1.2±0.1 to 1.9±0.3 viruses $cell^{-1}$ were on the surface of a bacterial cell on average per water sample. The abundance of viruses attached to prokaryotes (N_{VPR}) varied between 0.14 ×10^5 and 10.3 ×10^5 viruses mL^{-1}, averaging (1.6±0.1) × 10^5 viruses mL^{-1}. The average N_{VPR} value in CA (4.9±0.3 × 10^5 viruses mL^{-1}) was higher than in the Barents Sea (1.5 × 10^5 viruses mL^{-1}) and in MA (0.7±0.1 × 10^5 viruses mL^{-1}). The capsid diameter of viruses attached to prokaryotes varied from 16 to 167 nm. The average capsid diameters of viruses attached to prokaryotes per water sample varied between 45 and 88 nm, averaging 61±0.4 nm for all samples (Table 3).

The abundance of the pico-sized detrital particles with attached viruses (N_{PDV}) ranged between 0.6 ×10^5 до 4.2 ×10^5 particles mL^{-1} (on average 2.0±0.2 × 10^5 particles mL^{-1}) and was from 7.1% to 67.0% (on average 26.8±3.5%) of N_{PD} (Table 4, Fig. 2). The average N_{PDV} amount was 1.2 × 10^5 particles mL^{-1} in the Barents Sea, 1.8±0.3 ×10^5 particles mL^{-1} in MA and 2.4±0.4 × 10^5 particles mL^{-1} in CA. From 1 to 17 viruses were attached to the surface of a single detrital particle. As a result, the abundance of viruses attached to detrital particles (N_{VPD}) was (1.2−14.6) ×10^5 (on average 4.6±0.6 × 10^5) viruses mL^{-1}. The average abundance of N_{VPD} was 2.1 × 10^5 viruses mL^{-1} in the Barents Sea, 4.1±0.6 ×10^5 viruses mL^{-1} in MA and 5.9±1.2 × 10^5 viruses mL^{-1} in CA. The capsid diameter of viruses attached to detrital particles fluctuated between 21 and 137 nm. The average capsid diameters of viruses attached to PD per water sample were 25−72 nm, averaging 56±3 nm for all samples (Table 4).

As a result, the total abundance of virioplankton (N_{VT}) was (14-140) × 10^5 viruses mL^{-1}, averaging (62±6) × 10^5 viruses mL^{-1} (Fig. 3a). Thus, the proportion of free viruses in N_{VT} was 72.0−98.1 (on average 89.8±6.0) % and was significantly higher than the proportion of viruses attached to prokaryotes, 0.3−7.6 (on average 2.2±0.6) % and viruses attached to detrital particles 1.6−26.5 (on average 8.0±1.3) %. The largest contribution of free viruses to the N_{VT} formation was found at station 3 in MA, viruses attached to prokaryotic cells at station 12 in CA, viruses attached to detrital particles at station 23 in CA.

The total biomass of virioplankton (B_{VT}) varied between 0.08 and 0.77 mg C m^{-3}, averaging 0.33±0.03 mg C m^{-3}, and the proportion of virioplankton biomass of the prokaryotic biomass

(B_{VT}/B_{PR}) varied between 2.1 and 35.0% (on average 10.1±1.9%) (Fig. 3b, c). The B_{VT} and B_{VT}/B_{PR} values were, on average, 0.22 mg C m^{-3} and 3.2% in the Barents Sea; 0.11 mg C m^{-3} and 12.6% in the Kara Strait; 0.30±0.03 mg C m^{-3} and 15.4±0.9% in MA; 0.43±0.06 mg C m^{-3} and 4.2±0.3% in CA.

Viral infection and virus-mediated mortality of prokaryotes

The frequency of visibly infected prokaryotic cells (*FVIC*) ranged from 0.4 to 3.5% N_B, averaging 1.4±0.2% N_B (Table 5, Fig. 2). There was no significant positive correlation between N_{PR} and *FVIC*. Based on the *FVIC* estimation results, it was calculated that the proportion of virus-infected cells of N_{PR} (*FIC*) varied from 2.9 to 22.1% of N_{PR} (on average 9.2±0.9% of N_{PR}), and the viral-mediated mortality of prokaryotes (*VMPR*) was 4.0−34.0% (on average 11.4±1.5%) of the prokaryotic production (P_{PR}). The mortality of bacteria due to the viral-mediated lysis on average in the period of June 29–July 1(14.4±2.2 % P_{PR}) significantly exceeded that in the period of July 12–15 (7.6±1.8% P_{PR}).

The abundance of visibly infected prokaryotic cells (N_{PRVIC}) was (1–36) × 10^3 cells mL^{-1}, averaging 8±2 × 10^3 cells mL^{-1}. The minimum and maximum N_{PRVIC} / N_{PRV} ratio values differed by 7 times (Table 5) and the N_{PRV} / N_{PRVIC} ratio varied from 8 to 58. A high positive correlation was found between N_{PRV} and $N_{PRVIC,}$ r = 0.89, p <0.005, n = 21. If the average abundance of viral infected prokaryotic cells in MA was 6 times lower than in CA, the N_{PRVIC} / N_{PRV} values in these areas did not differ significantly, 5.8±1.0% и 4.9±1.1%, respectively.

The number of phages in viral-infected prokaryotic cells (*BS*) fluctuated from 4 to 35 phages $cell^{-1}$, averaging 7.1±0.7 phages $cell^{-1}$ (Table 5). The average *BS* values in the period of June 29–July 1 (7.0±0.8 viruses $cell^{-1}$) and July 12–15 (7.3±1.2 viruses $cell^{-1}$) were close.

Cocci+ellipsoid cells (58–71%) made the main contribution to the formation of the total abundance of prokaryotes, rods and vibrios (28−41%) and filaments (0−3.0%) were less abundant (Fig. 4a). Rods and vibrios accounted for the largest fraction of the virus-infected prokaryotes (69–94% of the total abundance of infected prokaryotes), with lower numbers observed for cocci, ellipsoids and filaments (6−28% and 0–3%) (Fig. 4b). That is, the phages infected prokaryotic cells of different morphology at a different rate. The fraction of the virus-infected rods and vibrios in the total abundance of prokaryotes of the respective morphology was the highest in the Barents Sea. The fraction of virus-infected cocci and ellipsoids in the total abundance of prokaryotes of the respective morphology was the lowest in CA. The frequency of occurrence of virus infection in cocci and ellipsoids in the MA was higher than in the CA, but the frequency of occurrence of virus infection in cocci and ellipsoids in MA was lower than in CA (Fig. 4c).

DISCUSSION

Abundance and biomass of viruses

The comparison of the results of studies of planktonic viruses on the Kara Sea shelf conducted at different times of the year showed that in summer, the average N_{VF} (59±5 × 10^5 viruses mL^{-1}) and N_{VF}/N_{PR} (23.9±4.9) values were higher than those obtained in early spring, 10.8±1.5 × 10^3 viruses mL^{-1} and 6.9±0.8 (Kopylov et al., 2019) and in autumn, 17.3±4.8 × 10^3 viruses mL^{-1} and 5.0±0.5 (Kopylov et al., 2015; Kopylov et al., 2017). The abundance of free viruses in the Kara Sea are within the range of N_{VF} ((0.1−64.1) × 10^6 viruses mL^{-1}) and N_{VF}/N_B (0.8−70.0%) values recorded in the central Arctic Ocean and other Arctic seas (Steward, Smith & Azam, 1996; Hodges et al., 2005; Steward et al., 2007; Clasen et al., 2008; Venger e t al., 2016).

In summer, the average proportion of virioplankton biomass of the prokaryotic biomass in Kara Strait and Kara Sea was 10.7±4.7%. In early spring, the role of viruses in the formation of the plankton microbial community biomass was less significant, B_V was only 2.2±1.3% of B_{PR}. For comparison, the viral biomass in the central Arctic Ocean is about 6% of the prokaryotic biomass (Steward et al., 2007).
In summer and spring, on the shelf of the Kara Sea, as in other marine ecosystems (Steward, Smith & Azam, 1996; Auguet et al., 2005), high positive correlations were found between N_{VF} and N_{PR}, that, apparently, indicates a significant amount of bacteriophages in the virioplankton composition (Wommack & Colvell, 2000).

Size of viruses

In aquatic environments pelagic viruses with a capsid size between 30 and 70 nm are the most abundant while larger viruses (>80 nm) are more rare (Cochlan et al., 1993; Berg et al., 1989; Wommack & Colvell, 2000; Alonso et al., 2001; Auguet et al., 2006).This indicates that the majority of viruses present in aquatic environments are most likely bacteriophages, as they have an average capsid-size of 70 nm (Cochlan et al., 1993; Wommack & Colvell, 2000; Alonso et al., 2001). Viruses of eukaryotic algae have an average capsid size of 152 nm (Van Etten, Lane & Meints, 1991).
The majority of pelagic viruses in surface waters on the Kara Sea Shelf were less than 60 nm in diameter. Moreover, in summer, the proportion of viral particles with a capsid diameter <100 nm (mainly bacteriophages) of N_{VF} (95.97%) is higher than in spring (80.4%) and, conversely, the proportion of viruses with a capsid diameter >100 nm (hosts of which are mainly algae and other eukaryotic organisms) is significantly lower in summer (3.9%) than in spring (19.6%). As a result, the average capsid diameter of viruses in the summer of 2018 (51.9±1.3 nm) was 1.5 times lower than in the spring of 2016 (78.9±2.6 nm) (Kopylov et al., 2019). The presence of a large number of phycoviruses in the waters of the Kara Sea shelf in the early spring of 2016 is, apparently, due to the end of the diatom bloom on the lower surface of the ice. This was evidenced by both the appearance of the lower edge of the ice, colored brown, and the remains of characteristic colonies of ice algae (mainly *Nitzshia frigida*) in surface water samples. In addition, during this period, the bloom of *Phaeocystis pouchetii* began, already forming numerous colonies (Sazhin et al., 2017).

Viral infection and virus-mediated mortality of prokaryotes

In Arctic waters, the *FVIC* and *VMPR* values most often vary from 0.5% (range, 0−1.4%) of N_{PR} and 3.7 (range 0−10.6) % of R_{PR} (central Arctic region)(Steward et al., 2007) to 2.1 (range 0.3−5.2)% N_{PR} and 20.2 (range 2.2−57.9) % of R_{PR} (coastal waters of the Novaya Zemlya archipelago), respectively (Venger et al., 2016). Thus, in summer, the average *FVIC* and *VMPR* values in surface waters on the Kara Sea shelf are in the middle of the range of values determined in different regions of the Arctic (Steward, Smith & Azam, 1996; Middelboe, Nielsen & Bjørnsen, 2002; Boras et al., 2010).
As is known, the frequency of contacts between viral particles and prokaryotic cells depends on their respective abundance, the physical and chemical parameters of the water, as well as on the size of a given prokaryotic cell and a given viral capsid (Murray & Jackson, 1992). Apparently, the relatively larger size of rods and vibrios (from 0.6 × 0.2 μm to 1.7 × 0.6 μm) and filamentous prokaryotes (from 1.1 × 0.3 μm to 2.7 × 0.8 μm) compared to the cocci+ellipsoids cell (from 0.3 × 0.2 μm to 1.0 × 0.6 μm), contributes to a higher frequency of contacts between these

morphological types of prokaryotes and viruses and, as a consequence, to the higher probability of viral infection of these prokaryotes.

A high concentration of the pico-sized detrital particles (PD) with a size of less than 4 μm was found in the surface waters of the Kara Sea shelf; their abundance on average ($10.4\pm1.5 \times 10^5$ particles mL^{-1}) significantly exceeded the abundance of prokaryotes ($1.7\pm0.5\times 10^5$ cells mL^{-1}). As a result, the average abundance of detrital particles with attached viruses was close to that of prokaryotes. Apparently, the adsorption of viral particles to the pico-sized detrital particles reduced both the abundance of free viruses and the level of viral infection of prokaryotes. A negative correlation was found between the abundance of PD and *FVIC* $r = -0.67$, $p = 0.0008$, $n = 18$.

By adsorption to non-living organic particles, the viruses are thus, at least temporarily, not available for infecting new host cells and adsorption of viruses to organic particles is expected to have had a profound inhibitory effect on virally mediated mortality of microorganisms (Brussaard, Kuipers & Veldhuis, 2005; Mojica & Brussaard, 2014).

The low abundance of viruses during the transitional period from spring to summer is explained by the adsorption of viruses to inorganic suspended particles entering the coastal waters of Arctic Seas with run-off from adjacent land and to detrital particles formed in large quantities after phytoplankton bloom (Schoemann et al., 2005).

Recently, it was experimentally demonstrated that different virus populations strongly adsorb to gracier-derived fine-sediment. Moreover, the production of progeny was strongly delayed in the presence of glacier sediment (Maat, Prins & Brussaard, 2019; Maat, Visser & Brussaard, 2019).

In CA, the abundance and biomass of prokaryotes were significantly higher than in MA. At the same time the abundance of viruses in these zones did not differ significantly. As a result, the average N_{FV}/N_{PR} value in CA was by 4.9 times lower than in MA. The low viral abundance generally observed in the presence of high suspended particle load might be caused by adsorption to suspended particles (Simon et al., 2002). Apparently, higher concentrations of organic and mineral particles (including those with a size of less than 4 μm) entering CA in large amounts with runoff of the Ob and Yenisei rivers and correspondingly, higher adsorption of viruses to these particles resulted in reduced abundance of free-living viruses and also in low viral to prokaryotic ratio. Lower N_{FV}/N_{PR} values translate into lower contact rates between prokaryotes and viruses, reducing prokaryotic mortality.

CONCLUSIONS

In late June–early July (that is, at the end of the phenological spring-early summer), viruses are an essential component of the planktonic microbial community on the shelf of the Kara Sea, averaging about 10% of the prokaryotic biomass. The abundance of free viruses was higher than of those found on the Kara Sea shelf in early spring and autumn. A high positive correlation was found between the abundance of prokaryotes and the abundance of free viruses, which indicates a significant amount of bacteriophages in the virioplankton composition. A large number of viruses was attached to detrital particles with a size of 0.25-4.0 μm. The proportion of viruses attached to detrital particles of the total abundance of virioplankton dominated by free viruses was higher than the proportion of viruses attached to prokaryotic cells. The negative correlation between the frequency of virus-infected prokaryotic cells and the abundance of pico-sized detrital particles suggests that the latter are an important factor reducing the level of viral infection of prokaryotes. In the presence of differences in the structural characteristics of virioplankton in the western Marine Area and in the eastern Coastal Area, the level of viral

infection of heterotrophic prokaryotes in these zones was close. According to the obtained values of viral-mediated mortality of prokaryotes, in early summer, planktonic viruses, in general, play an essential role in controlling the abundance of prokaryotes on the Kara Sea shelf.

ACKNOWLEDGEMENTS

The authors would like to thank the employees of the Centre for Electron Microscopy of the Papanin Institute for Biology of Inland Waters of the Russian Academy of Sciences S.I. Metelev, G. Bykov, and Z. Bykova for their help in preparing the material for electron microscopy.

ADDITIONAL INFORMATION AND DECLARATIONS

Funding

The research was supported by Russian Science Foundation project no. 22-17-00011.

Grant Disclosures: htpps://rscf.ru/project/22-17-00011

Competing Interests

The authors declare there are no competing interests.

Author Contribution

Alexander I. Kopylov conceived and designed the experiments, performed the experiments, wrote the paper, prepared tables and approved the final draft.
Elena A. Zabotkina conceived and designed the experiments, performed the experiments, analyzed the data, prepared figures, reviewed drafts of the paper and approved the final draft.
Andrey F. Sazhin conceived and designed the experiments, performed the experiments, analyzed the data and approved the final draft.
Nadezda D. Romanova conceived and designed the experiments, performed the experiments, analyzed the data and approved the final draft.
Anastasia M. Drozdova and Nicolay A. Belyaev performed the experiments, analyzed the data and approved the final draft.

REFERENCES

Alonso MC, Jimenez-Gomez F, Rodriguez J, Borrego JJ. 2001. Distribution of virus-like particles in an oligotrophic marine environment (Alboran sea, Western Mediterranean). *Microbial Ecology* 42: 407−415 DOI: 10.1007/s00248-001-0015-y.

Auguet JC, Montanié H, Delmas D, Hartmann HJ, Huet V. 2005. Dynamic virioplankton abundance and its environmental control in the Charente estuary (France). *Microbial Ecology* 50: 337−349 https://doi.org/10.1007/s00248-005-0183-2.

Auguet JC, Montanié H, Lebaron P. 2006 Structure of virioplankton in the Charente Estuary (France): transmission electron microscopy versus pulsed field gel electrophoresis. *Microb. Ecol.* 51: 197–208.

Belyaev NA, Peresypkin VI, Ponyaev MS. 2010. The organic carbon in the water, the particulate matter, and the upper layer of the bottom sediments of the west Kara Sea. *Oceanology* 50: 706–715 https://doi.org/10.1134/S0001437010050085.

Bettarel I, Sime-Ngando T, Amblard C, Laveran H. 2000. A comparison of methods for counting viruses in aquatic systems. *Applied Environmental Microbiology* 66: 2283−2289 DOI: 10.1128/aem.66.6.2283-2289.2000.

Boras JA, Sala MM, Arrieta JM, Sa EL, Felipe J, Agustí S, Duarte CM, Vaqué D. 2010. Effect of ice melting on bacterial carbon fluxes channeled by viruses and protists in the Arctic Ocean. *Polar Biology* 33: 1695−1707 https://doi.org/10.1007/s00300-010-0798-8.

Binder B. 1999. Reconsidering the relationship between virally induced bacterial mortality and frequency of infected cells. *Aquatic Ecology* 18: 207−215 DOI:10.3354 /AME018207.

Bratbak G, Thingstad TF, Heldal M. 1994. Viruses and the microbial loop. *Microbial Ecology* 28: 209−221 https://doi.org/10.1007/BF00166811.

Brussaard CPD, Kuipers B, Veldhuis MJW. 2005. A mesocosm study of Phaeocystis globosa population dynamics – I. Regulatory role viruses in bloom control. *Harmful Algae* 4: 859–874 https://doi.org/10.1016/j.hal.2004.12.015.

Clasen JL, Brigden SM, Payet JP, Suttle CA. 2008. Evidence that viral abundance across oceans and lakes is driven by different biological factors. *Freshwater Biology* 53: 1090–1100 https://doi.org/10.1111/j.1365-2427.2008.01992.x.

Cochlan WP, Wikner J, Steward GF, Smith DC, Azam F. 1993. Spatial distribution of viruses, bacteria and chlorophyll a in neretic, oceanic and estuarine environments. *Marine Ecology Progress Series* 92: 77−87.

Guixa-Boixereu N, Vaqué D, Gasol JM, Sánchez-Cámara J, Pedrós-Alió C. 2002. Viral distribution and activity in Antarctic waters. *Deep Sea Research II* 49: 827–845 https://doi.org/10.1016/S0967-0645(01)00126-6.

Hammer Ø, Harper DA, Ryan PD. 2001. PAST: Paleontological statistics software package for education and data analysis. *Palaeontologia electronica* 4(1) 4: 9.

Hodges LR, Bano N, Hollibaugh JT, Yager P. 2005. Illustraing the importance of particulate organic matter to pelagic microbial abundance and community structure – an Arctic case study. *Aquatic Microbial Ecology* 40: 217–227 DOI: 10.3354/ame040217.

Kopylov AI, Zabotkina EA, Sazhin AF, Romanova ND. 2015. Virioplankton in the Kara Sea: the impact of viruses on mortality of heterotrophic bacteria. *Oceanology* 55(4): 561–572 https://doi.org/10.1134/S0001437015040104.

Kopylov AI, Zabotkina EA, Romanenko AV, Sazhin AF, Romanova ND. 2017. Virio- and bacterioplankton in the estuary zone of the Ob River and adjacent regions of the Kara Sea shelf. *Oceanology* 57(1):105–113 https://doi.org/10.1134/S0001437017010052.

Kopylov AI, Sazhin AF, Zabotkina EA, Romanenko AV, Romanova ND, Boltenkova MA. 2019. Virioplankton of the Kara Sea and the Yenisei River estuary in early spring. *Estuarine, Coastal and Shelf Science* 217: 37–44 https://doi.org/10.1016/j.ecss.2018.10.015.

Lasareva EV, Parfenova AM, Romankevich EA, Lobus NV, Drozdova AN. 2019. Organic matter and mineral interections modulate flocculation across arctic river mixing zones. *JGR Biogeosciences* 124: 1651 – 1664 https://doi.org/10.1029/2019jg005026.

505 Maat DS, Prins MA, Brussaard CPD. 2019. Sediments from Arctic tide-water glaciers remove
506 coastal marine viruses and delay host infection. *Viruses* 11(2): 123
507 https://doi.org/10.3390/v11020123.

508 Maat DS, Visser RJW, Brussaard CPD. 2019. Virus removal by gracier-derived suspended fine
509 sediment in the Arctic. *Journal of Experimental Marine Biology and Ecology* 521: 151227
510 https://10.1016/j.jembe.2019.151227.

511 Makkaveev PN, Melnikova ZG, Polukhin AA, Stepanova SV, Khlebopashev PV, Chultsova AL.
512 2015. Hydrochemical characteristics of the waters in the western part of the Kara Sea.
513 *Oceanology* 55(4): 485−496 DOI: 10.1134/S0001437015040116.

514 Maranger R, Vaqué D, Nguyen D, Hébert MP, Lara E. 2015. Pan-Arctic patterns of
515 planktonic heterotrophic microbial abundance and processes: controlling factors and
516 potential impacts of warming. *Progress in Oceanography* 139: 221–232
517 https://doi.org/10.1016/j.pocean.2015.07.006.

518 Middelboe M, Nielsen TG, Bjørnsen PK. 2002. Viral and bacterial production in the north water
519 in situ measurements batch-culture experiments and characterization of a viral-host system. *Deep*
520 *Sea Research Part II: Topical Studies in Oceanography* 49: 5063−5079
521 https://doi.org/10.1016/S0967-0645(02)00178-9.

522 Mostajir B, Dolan J, Rassoulzadegan F. 1995. A simple method for the quantification of a class a
523 labile marine pico- and nano-sized detritus: DAPI Yellow Particles (DYP). *Aquatic Microbial*
524 *Ecology* 9: 259–266 https://doi.org/10.3354/ame009259.

525 Mojica KDA; Brussaard CPD. 2014. Factors affecting virus dynamics and microbial host-virus
526 interactions in marine environments. *FEMS Microbiology Ecology* 89: 495−515
527 https://doi.org/10.1111/1574-6941.12343.

528 Murray AG, Jackson GA. 1992. Viral dynamics: a model of the effects of size, shape,
529 motion and abundance of single-celled planktonic organisms and other particles. *Marine*
530 *Ecology Progress Series* 89: 103–116 https://doi.org/10.3354/meps089103.

531 Noble RT, Fuhrman JA. 1998. Use of SYBR Green for rapid epifluorescence count of marine
532 viruses and bacteria. *Aquatic Microbial Ecology* 14: 113−118 DOI:10.3354/AME014113.

533 Norland S. 1993. The relationship between biomass and volume of bacteria. In: Kemp PF, Sherr
534 BF, Sherr EB, Cole JJ, eds. *Handbook of Methods in Aquatic Microbial Ecology* Boca Raton:
535 Lewis Publ. 303–308.

536 Porter KG, Feig YS. 1980. The use DAPI for identifying and counting of aquatic microflora.
537 *Limnology and Oceanography* 25(5): 943−948 https://doi.org/10.4319/lo.1980.25.5.0943.

538 Proctor LM, Okubo A, Fuhrman JA. 1993. Calibration estimates of phage-induced mortality in
539 marine bacteria: ultrastructural studies of marine bacteriophage development from one-step
540 growth experiments. *Microbial Ecology* 25: 161−182 https://doi.org/10.1007/BF00177193.

541 Romanova ND., Boltenkova MA. 2020. Seasonal variability of bacterioplankton of the Yenisei
542 Estuary. *Oceanology* 60(1): 74−82 DOI: 10.1134/S0001437020010191.

543 Romanova ND, Boltenkova MA, Polukhin AA, Bezzubova EM, Shchuka SA. 2022.
544 Heterotrophic bacteria of the Ob River Estuary during Groving season: Spatial and Temporal
545 variability. *Oceanology* 62: 369−378 https.//doi.org/10.1134/s000143/022030109.

Sazhin AF, Mosharov SA, Romanova ND, Belyaev NA, Khlebopashev PV, Pavlova MA, Druzhkova EI, Flint MV, Kopylov AI, Zabotkina EA, Ishkulov DG, Makarevich PR, Pasternak AF, Makkaveev PN, Drozdova AN. 2017. The plankton community of the Kara Sea in early spring. *Oceanology* 57: 222–224 https://doi.org/10.1134/S0001437017010179.

Sandaa R-A, Storesund JE, Olesin E, Paulsen ML, Larsen A, Bratbak G, Ray JL. 2018. Seasonality drives microbial community structure, shaping both eukaryotic and prokaryotic host–viral relationships in an arctic marine ecosystem. *Viruses* 10: 715 https://doi.org/10.3390/v10120715.

Schoemann V, Becquevort S, Stefels J, Rousseau W, Lancelot C. 2005. *Phaeocystis* blooms in the global ocean and their controlling mechanisms: a review. *Journal of Sea Research* 53: 43–66 https://doi.org/10.1016/j.seares.2004.01.008.

Simon M, Grossart HP, Schweitzer B, Ploug H. 2002. Microbial ecology of organic aggregates in aquatic ecosystems. *Aquatic Microbial Ecology* 28: 175−211 DOI:10.3354/ame028175.

Steward GF, Fandino LB, Hollibaugh JT, Whitledged TE, Azam F. 2007. Microbial biomass and viral infections of heterotrophic prokaryotes in the sub-surface layer of the Central Arctic Ocean. *Deep Sea Research Part I: Oceanographic Research Papers* 54: 1744−1757 https://doi.org/10.1016/j.dsr.2007.04.019.

Steward GF, Smith DC, Azam F. 1996. Abundance and production of bacteria and viruses in the Bering and Chukchi Seas. *Marine Ecology Progress Series* 131: 287−300 DOI:10.3354/meps131287.

Suttle CA. 1993. Enumeration and isolation of virus. In: Kemp PF, Sherr BF, Sherr EB, Cole JJ, eds. *Handbook of Methods in Aquatic Microbial Ecology* Boca Raton: Lewis Publ, 121−134.

Suttle CA. 2007. Marine viruses – major players in the global ecosystem. *Nature Reviews Microbiology* 5: 801–812 https://doi.org/10.1038/nrmicro1750.

Van Etten JL, Lane LG, Meints RH. 1991. Viruses and virus like particles of eukaryotic algae. *Microbiological Reviews* 55(4): 586−620. DOI:10.1128/MMBR.55.4.586-620.1991.

Venger MP, Kopylov AI, Zabotkina EA, Makarevich PR. 2016. The influence of viruses on bacterioplankton of the offshore and coastal parts of the Barents Sea. *Russian Journal of Marine Biology* 42(1): 26–35 https://doi.org/10.1134/S106307401601017X.

Wells LE, Deming JW. 2003. Abundance of Bacteria, the Cytophaga-Flavobacterium cluster and Archaea in cold oligotrophic waters and nepheloid layers of the Northwest Passage, Canadian Archipelago. *Aquatic Microbial Ecology* 31: 19−31 https://doi.org/10.3354/ame031019.

Wells LE, Deming JW. 2006a. Characterization of cold-active bacteriophage on two psychrophilic marine hosts. *Aquatic Microbial Ecology* 45: 15–29 DOI:10.3354/ame045015.

Wells LE, Deming JW. 2006b. Significance of bacterivory and viral lysis in bottom waters of Franklin Bay, Canadian Arctic, during winter. *Aquatic Microbial Ecology* 43: 209−221 DOI:10.3354/ame043209.

Weinbauer MG, Brettar L, Höfle MG. 2003. Lysogeny and virus-induced mortality of bacterioplankton in surface, deep, and anoxic marinewaters. *Limnology and Oceanography* 48: 1457−1465 https://doi.org/10.4319/lo.2003.48.4.1457.

587 Weinbauer MG, Rassoulzadegan F. 2004. Are viruses driving microbial diversification and
588 diversity? *Environmental Microbiology* 6: 1–11 https://doi.org/10.1046/j.1462-
589 2920.2003.00539.x.

590 Wilhelm SW, Suttle CA. 1999. Viruses and nutrient cycles in the sea. *Bioscience* 49: 781−788
591 https://doi.org/10.2307/1313569.

592 Wommack KE, Colvell RR. 2000. Virioplankton: Viruses in Aquatic Ecosystems. *Microbiology*
593 *and Molecular Biology Reviews* 64: 69−114. https://doi.org/10.1080/19475721003743843.

Figure 1

The scheme of the locations of the sampling stations

black circles denote stations samples were taken on June 29 – July 1, 2018; <!--[if !vml]--> <!--[endif]--> white triangles denote stations samples were taken on July 12–15, 2018.

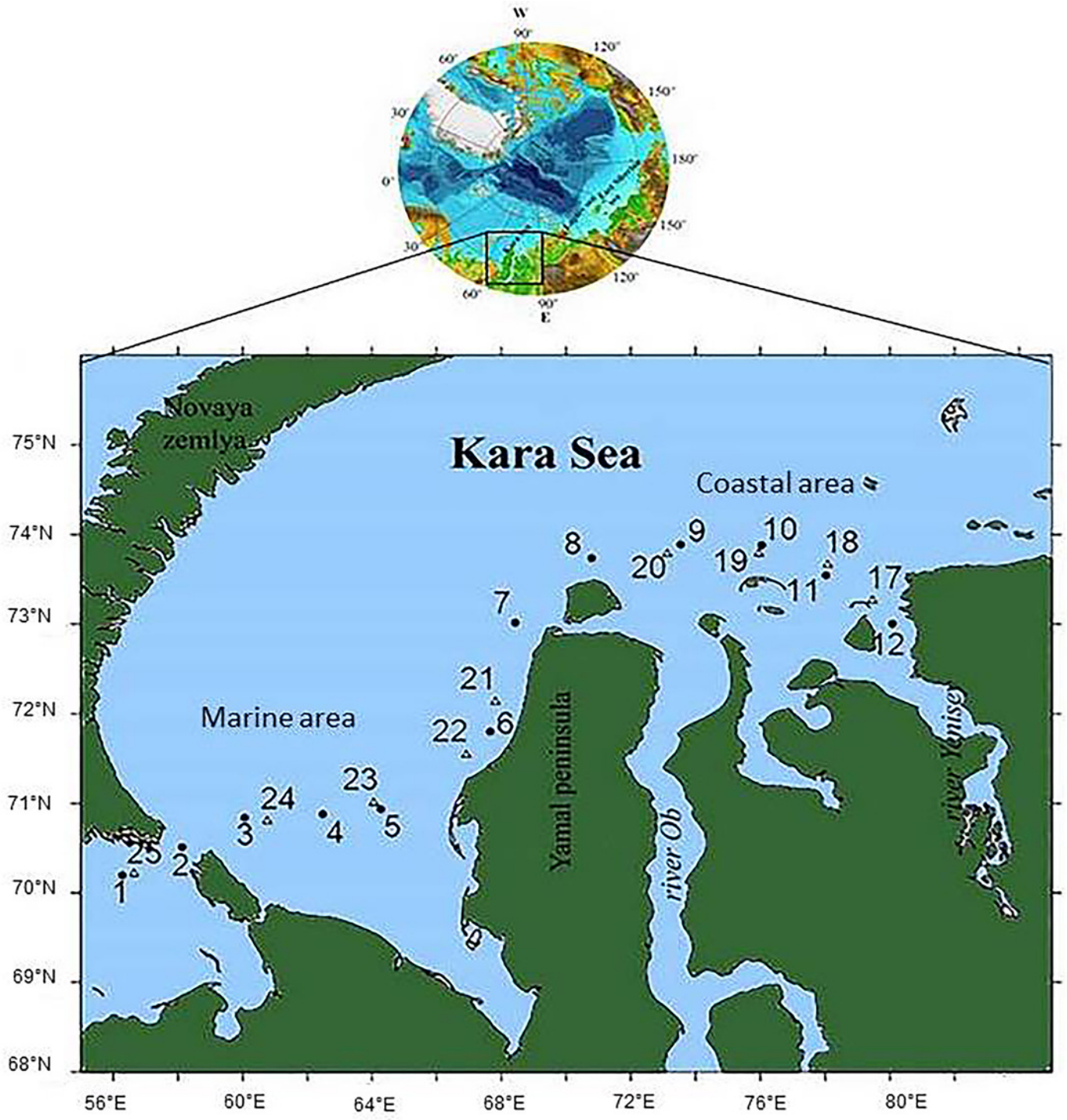
Novaya zemlya
Kara Sea
Coastal area
Marine area
Yamal peninsula
river Ob
river Yenisei
1
2
3
4
5
6
7
8
9
10
11
12
17
18
19
20
21
22
23
24
25
75°N
74°N
73°N
72°N
71°N
70°N
69°N
68°N
56°E
60°E
64°E
68°E
72°E
76°E
80°E

Figure 2

Electron micrographs of viruses in shelf waters of the Kara Sea

(A – D) free virus particle, (E, G) prokaryotes with viruses on surface, (E, F, G) virus-infected prokaryotes − viruses inside cell, (H, I) viruses attached to detrital particle

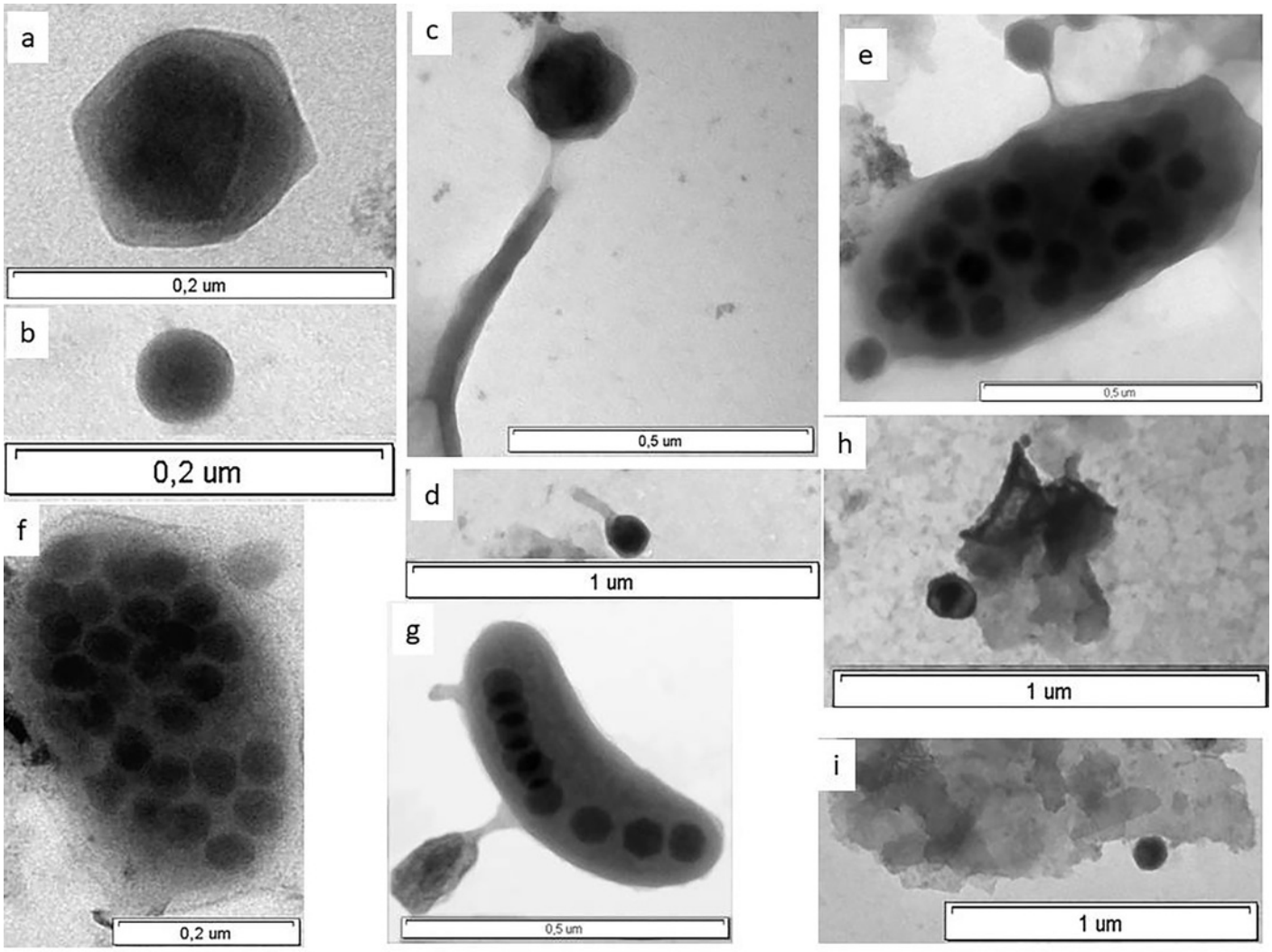

Figure 3

Abundance and biomass of virioplankton in the surface water layer in Arctic Seas

(A) abundance of virioplankton, (B) biomass of virioplankton, (C) virioplankton biomass / prokaryotic biomass ratio

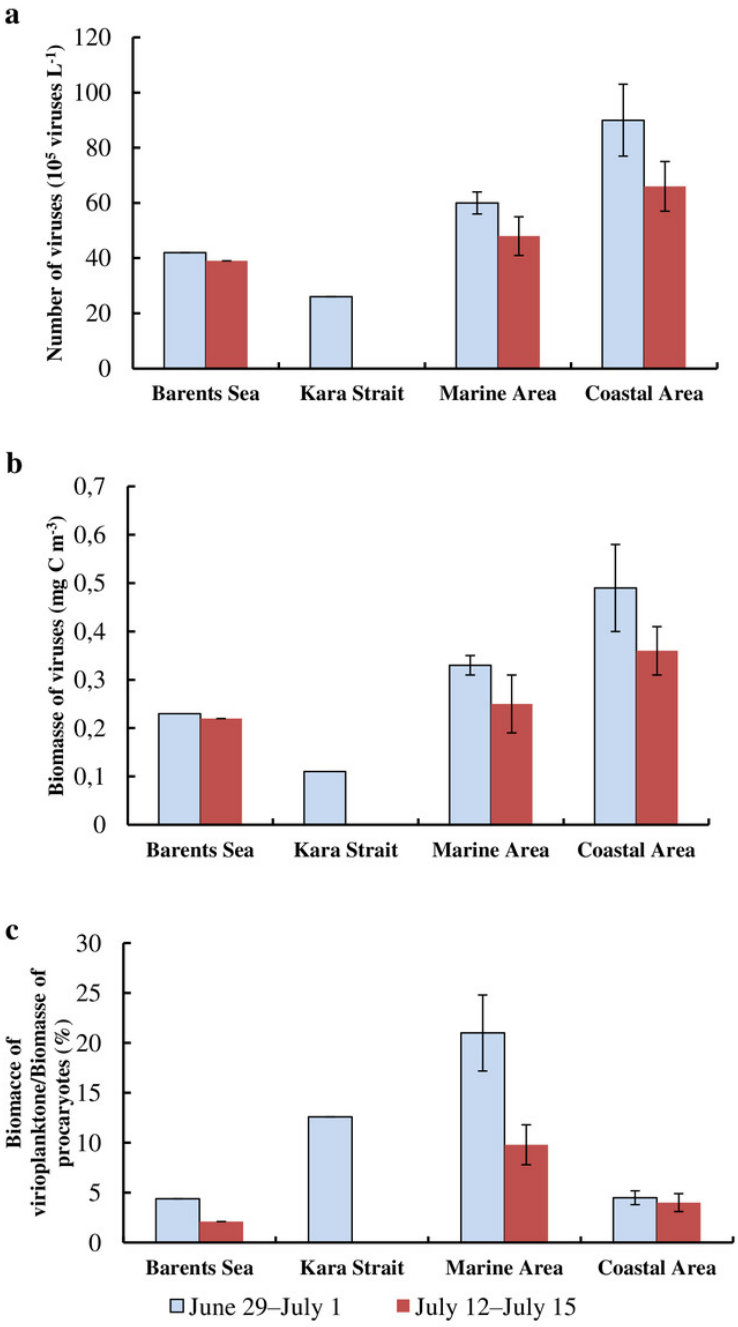
a
Number of viruses (10^5 viruses L^{-1})
120
100
80
60
40
20
0
Barents Sea
Kara Strait
Marine Area
Coastal Area
b
Biomasse of viruses (mg C m^{-3})
0,7
0,6
0,5
0,4
0,3
0,2
0,1
0
Barents Sea
Kara Strait
Marine Area
Coastal Area
c
Biomacce of virioplanktone/Biomasse of procaryotes (%)
30
25
20
15
10
5
0
Barents Sea
Kara Strait
Marine Area
Coastal Area
June 29–July 1
July 12–July 15

Figure 4

Share of prokaryotic cells of various morphology to the total abundance of prokaryotes (A), share of infected prokaryotic cells of various morphology to the total number of infected prokaryotic cells (B), share of infected prokaryotic cells of various mor

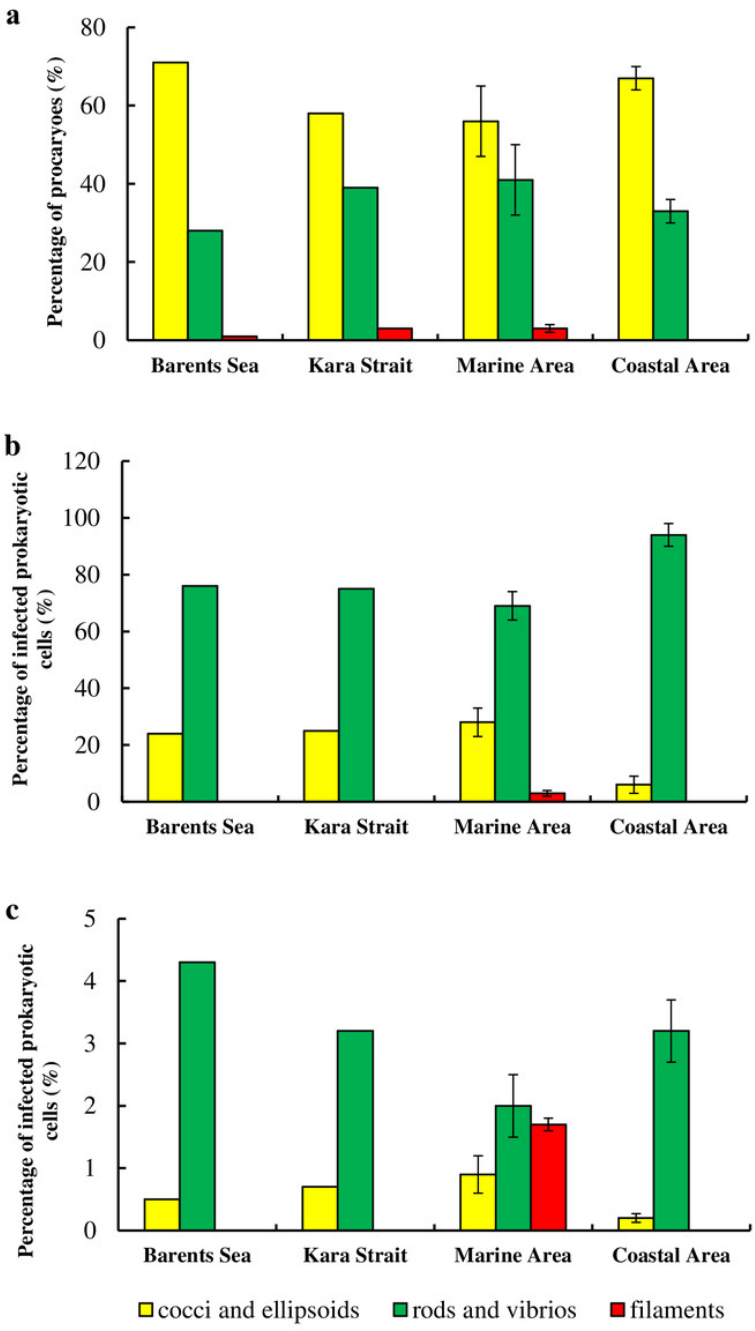
a
Percentage of procaryoes (%)
80
60
40
20
0
Barents Sea
Kara Strait
Marine Area
Coastal Area
b
Percentage of infected prokaryotic cells (%)
120
100
80
60
40
20
0
Barents Sea
Kara Strait
Marine Area
Coastal Area
c
Percentage of infected prokaryotic cells (%)
5
4
3
2
1
0
Barents Sea
Kara Strait
Marine Area
Coastal Area
cocci and ellipsoids
rods and vibrios
filaments

Table 1(on next page)

Temperature (*T*), salinity (*S*), concentration of dissolved organic carbon in water (*DOC*), abundance (N_{PR}) and biomass (B_{PR}) of prokaryotes in the surface water layer on the Kara Sea shelf in the summer of 2

* samples were taken on June 29 – July 1, 2018, ** samples were taken on July 12–15, 2018

Table 1. Temperature (*T*), salinity (*S*), concentration of dissolved organic carbon in water (*DOC*), abundance (N_{PR}) and biomass (B_{PR}) of prokaryotes in the surface water layer on the Kara Sea shelf in the summer of 2018

Stations	*T*, °C	*S*, psu	*DOC*, mg L^{-1}	Prokaryotes	
				N_{PR}, 10^5 cells mL^{-1}	B_{PR}, mg C m^{-3}
Barents Sea					
1*	6.4	28.98	2.62	5.3	5.26
25**	8.9	29.70	2.92	10.0	10.59
Kara Strait					
2*	1.2	33.42	1.42	0.7	0.87
Marine area, Kara Sea					
3*	-0.73	27.12	1.39	0.9	1.74
4*	-1.00	26.93	2.34	0.8	1.24
5*	1.6	30.41	1.66	0.6	0.82
6*	2.1	31.92	2.11	1.3	1.51
7*	1.9	32.23	2.38	2.2	2.44
8*	1.4	30.22	3.94	4.6	4.95
21**	4.8	30.67	3.30	3.0	4.23
22**	2.5	32.00	2.13	1.4	2.14
23**	2.4	32.56	1.98	1.9	2.80
24**	1.5	32.80	1.62	1.7	1.73
Coastal area, Kara Sea					
9*	3.9	15.48	7.93	7.4	5.59
10*	3.2	14.00	5.87	8.3	9.39
11*	5.1	4.9	11.46	8.4	8.63
12*	7.9	0.25	9.64	25.3	27.68
17**	7.1	2.17	9.48	11.8	13.07
18**	6.9	13.48	7.85	18.7	20.34
19**	4.0	11.06	9.36	7.7	8.07
20**	3.4	25.13	6.96	3.5	4.45

* samples were taken on June 29 – July 1, 2018, ** samples were taken on July 12–15, 2018.

Table 2 (on next page)

Abundance of free viruses (N_{VF}), ratio of abundance of free viruses to abundance of prokaryotes (N_{VF}/N_{PR}), capsid diameter of free viruses (D_{VF})

* epifluorescence microscopy, ** transmission electron microscopy

Table 2. Abundance of free viruses (N_{VF}), ratio of abundance of free viruses to abundance of prokaryotes (N_{VF}/N_{PR}), capsid diameter of free viruses (D_{VF})

Station	N_{VF}, 10^5 viruses mL^{-1}		N_{VF}/N_{PR}	D_{VF}, nm	
	EM*	TEM**		Mean±SE	Min-max
Barents Sea					
1	37	25	7.0	38±1	18−76
25	36	27	3.7	53±2	16−155
Kara Strait					
2	21	39	29.4	48±3	17−196
Marine area, Kara Sea					
3	53	65	57.2	52±2	23−106
4	63	55	77.0	64±3	26−177
5	47	60	73.0	61±3	16−155
6	37	25	29.4	54±2	21−129
7	68	60	30.7	49±3	26−304
8	66	47	14.6	47±1	16−80
21	74	51	24.7	50±2	16−205
22	40	31	28.9	42±2	16−133
23	10	18	5.2	57±2	21−155
24	50	35	29.8	50±2	16−155
Coastal area, Kara Sea					
9	38	27	5.2	48±2	17−115
10	51	53	6.2	54±2	20−123
11	103	69	12.3	62±3	17−184
12	117	88	4.6	53±2	16−194
17	57	41	4.8	46±2	16−133
18	82	69	4.4	54±3	16−202
19	36	31	4.7	47±2	19−150
20	63	52	18.2	45±2	16−124

* epifluorescence microscopy, ** transmission electron microscopy

Table 3 (on next page)

Abundance of prokaryotes with attached viruses (N_{PRV}), proportion of prokaryotes with attached viruses of the total abundance of prokaryotes (N_{PRV}/N_{PR}), abundance of viruses on the surface of a single prokaryotic

Table 3. Abundance of prokaryotes with attached viruses (N_{PRV}), proportion of prokaryotes with attached viruses of the total abundance of prokaryotes (N_{PRV}/N_{PR}), abundance of viruses on the surface of a single prokaryotic cell (N_{VPR}/N_{PRV}), abundance of viruses attached to prokaryotes, (N_{VPR}), average capsid diameter of viruses attached to prokaryotes (D_{VPR})

Station	N_{PRV}, 10^5 cells mL^{-1}	N_{PRV}/N_{PR}, %	N_{VPR}/N_{PRV}, viruses $cell^{-1}$	N_{VPR}, 10^5 viruses mL^{-1}	D_{VB}, nm	
					Mean±SE	min-max
Barents Sea						
1	1.0	18.20	1.5±0,9	1.5	50±1	29–74
25	1.2	12.50	1.2±0.5	1.5	62±1	46–93
Kara Strait						
2	1.4	19.38	1.6±1.3	2.2	50±1	24–68
Marine area, Kara Sea						
3	0.2	23.5	1.5±0.8	0.3	60±3	22–90
4	0.2	26.9	1.4±1.2	0.3	78±1	65–101
5	0.2	30.5	1.5±0.8	0.3	62±1	47–79
6	0.3	22.9	1.5±0.7	0.4	63±1	36–89
7	0.7	32.6	1.9±1.4	1.4	70±2	41–139
8	1.0	20.9	1.5±1.0	1.4	56±2	22–77
21	0.7	22.3	1.7±1.2	1.1	66±2	43–97
22	0.3	24.7	1.6±1.1	0.5	45±2	27–97
23	0.2	10.9	1.7±1.3	0.4	47±1	31–63
24	0.4	26.5	1.5±0.8	0.7	65±1	42–92
Coastal area, Kara sea						
9	2.1	28.1	1.6±1.1	3.4	88±2	55–120
10	1.6	19.0	1.4±0.8	2.2	64±2	39–113
11	2.2	26.3	1.3±0.6	2.9	71±3	25–147
12	10.3	40.7	1.5±0.7	15.4	69±4	27–169
17	3.3	27.9	1.4±0.6	4.6	50±1	36–66
18	5.2	27.9	1.6±1.0	8.3	58±2	37–96
19	1.6	21.2	1.3±0.5	2.1	61±2	32–110
20	0.7	20.8	1.5±0.7	1.1	49±1	32–67

Table 4(on next page)

Abundance of detrital particles with attached viruses (N_{PDV}), diameter of detrital particles (D_{PD}), average number of viruses on a single particle (N_{VPD}/N_{PDV}), abundance of viruses attached to detr

Table 4. Abundance of detrital particles with attached viruses (N_{PDV}), diameter of detrital particles (D_{PD}), average number of viruses on a single particle (N_{VPD}/N_{PDV}), abundance of viruses attached to detrital particles (N_{VPD}), capsid diameter of a virus attached to particles (D_{VPD})

Station	N_{PDV}, 10^5 particles mL^{-1}	D_{PD}, µm		N_{VPD}/N_{PDV} viruses mL^{-1}	N_{VPD}, 10^5 viruses mL^{-1}	D_{VPD}, nm	
		min	max			Mean±SE	Min-max
Barents Sea							
1	1.5	0.25	3.0	2.1±1.5	3.2	48±1	30–67
25	1.0	0.45	3.5	1.1±0.5	1.1	25±1	25–45
Kara Strait							
2	2.0	0.25	4.0	2.6±1.3	5.2	55±2	39–84
Marine area, Kara Sea							
3	1.9	0.5	4.0	1.9±1.4	3.6	72±2	35–87
4	0.7	0.3	3.0	1.4±0.6	1.0	55±2	41–81
5	2.9	0.3	2.5	1.8±1.2	5.2	45±1	26–71
6	4.0	0.3	2.5	2.0±1.4	8.0	56±2	33–79
7	1.0	0.3	4.5	2.4±1.7	2.4	69±2	36–88
8	0.9	0.5	4.5	3.2±1.7	2.9	69±4	40–137
21	2.8	0.5	1.5	2.0±1.5	5.6	47±1	25–59
22	2.0	0.25	2.0	2.4±1.7	4.8	67±2	44–111
23	0.8	0.25	4.0	6.2±2.9	5.0	51±2	21–85
24	0.9	0.3	2.5	2.4±1.7	2.2	55±1	38–76
Coastal area, Kara Sea							
9	2.2	0.5	4.0	2.3±1.7	5.1	49±1	26–63
10	0.6	1.0	3.0	4.2±2.0	2.5	70±1	56–92
11	3.4	0.3	4.5	4.3±2.0	14.6	66±4	25–119
12	4.2	0.25	4.0	1.9±1.5	8.0	56±2	30–93
17	2.8	0.3	4.0	1.7±1.2	4.8	47±1	26–75
18	2.4	0.3	2.5	1.8±1.2	4.3	47±1	36–56
19	1.9	1.0	4.5	2.0±1.4	3.8	68±2	34–108
20	2.0	0.25	2.5	2.0±1.2	4.0	50±1	36–69

Table 5(on next page)

Frequency of visibly infected prokaryotic cells (*FVIC*), frequency of infected prokaryotic cells (*FIC*), virus-mediated prokaryotic mortality (*VMB*), number of mature phages inside prokaryotic cells (*BS*) and ratio of the abundance of

Table 5. Frequency of visibly infected prokaryotic cells (*FVIC*), frequency of infected prokaryotic cells (*FIC*), virus-mediated prokaryotic mortality (*VMB*), number of mature phages inside prokaryotic cells (*BS*) and ratio of the abundance of infected cells to the abundance of cells with attached viruses (N_{PRVIC}/N_{PRV}, %)

Station	*FVIC*, % от N_{PR}	*FIC*, % of N_{PR}	*VMPR*, % of P_{PR}	*BS*, viruses cell^{-1}		N_{PRVIC}/N_{PRV}
				Mean±SE	Max	
Barents Sea						
1	2.2	14.5	19.2	5.7±0.1	8	11
25	1.4	9.0	10.6	10.0±0.4	15	18
Kara Strait						
2	1.8	12.0	15.1	6.0±0.2	8	20
Kara Sea. Marine Area.						
3	1.9	12.7	16.1	7.0±0.2	11	17
4	1.3	8.8	10.4	6.0±0.2	9	28
5	1.4	9.0	10.6	6.0±0.3	11	28
6	0.4	2.8	2.9	4.0	4	147
7	3.5	22.1	34.0	5.0±0.2	9	14
8	1.2	8.2	9.5	5.8±0.3	10	26
21	0.8	5.5	6.1	6.0±0.2	8	56
22	0.8	5.5	6.1	6.3±0.1	8	40
23	1.2	8.2	9.5	17.0±0.7	24	30
24	1.2	8.2	9.5	5.5±0.1	7	42
Kara Sea. Estuarine Area						
9	1.0	6.9	7.8	6.3±0.2	9	40
10	2.5	16.3	22.3	9.4±0.8	32	10
11	1.4	10.1	12.2	15.2±1.1	35	26
12	1.4	10.1	12.2	7.0±0.3	11	37
17	0.7	4.9	5.4	5.0±0.1	6	28
18	1.0	6.9	7.8	5.3±0.1	6	31
19	1.0	6.9	7.8	5.3±0.1	7	11
20	0.7	4.9	5.4	5.4	6	26